Article published online: 2023-10-19

Intravital Imaging of Thrombosis Models in Mice

Klytaimnistra Kiouptsi[1,2] Martina Casari[1] Jonathan Mandel[1] Zhenling Gao[1] Carsten Deppermann[1,2]

[1] Center for Thrombosis and Hemostasis, University Medical Center of the Johannes Gutenberg University, Mainz, Germany
[2] German Center for Cardiovascular Research (DZHK), Partner Site Rhine-Main, Mainz, Germany

Address for correspondence Carsten Deppermann, PhD, Center for Thrombosis and Hemostasis (CTH), University Medical Center of the Johannes Gutenberg University Mainz, Langenbeckstraße 1, 55131 Mainz, Germany (e-mail: deppermann@uni-mainz.de).

Hamostaseologie 2023;43:348–359.

Abstract

Intravital microscopy is a powerful tool to study thrombosis in real time. The kinetics of thrombus formation and progression *in vivo* is studied after inflicting damage to the endothelium through mechanical, chemical, or laser injury. Mouse models of atherosclerosis are also used to induce thrombus formation. Vessels of different sizes and from different vascular beds such as carotid artery or vena cava, mesenteric or cremaster arterioles, can be targeted. Using fluorescent dyes, antibodies, or reporter mouse strains allows to visualize key cells and factors mediating the thrombotic processes. Here, we review the latest literature on using intravital microscopy to study thrombosis as well as thromboinflammation following transient middle cerebral artery occlusion, infection-induced immunothrombosis, and liver ischemia reperfusion.

Keywords
- thrombosis
- platelet
- microscopy
- intravital
- mice

Introduction

Intravital microscopy (IVM) is a powerful tool to study arterial or venous thrombosis in real time. To observe the dynamic thrombus formation and progression *in vivo*, damage is inflicted to the vascular endothelium through mechanical, chemical, or laser injury. Both vessels with large diameter such as carotid artery, femoral artery, or vena cava as well as small diameter, such as mesenteric or cremaster arterioles, can be targeted. Atherosclerotic mouse models offer to observe non–injury-induced thrombus formation. By introducing fluorescent dyes or fluorescently labeled antibodies, the researcher can label and visualize different components of the clotting process including platelets, leukocytes, fibrin, and other factors. The combination of such tools with genetic mouse models allows the identification of key players in thrombosis and to test novel therapeutic approaches.

In this review, we will summarize and discuss the role of intravital imaging in thrombosis models in various vascular beds. After reading this review, the reader should have gained an understanding of the thrombosis models available that can be combined with intravital microscopy to follow the cellular processes unfolding in real time and to serve their research question (►Fig. 1). A summary of the techniques discussed is provided in (►Table 1).

Arterial Thrombosis Models

Carotid Artery

The carotid artery injury is often used as a model to study arterial thrombosis *in vivo*. In these models, the injury can be induced mechanically, through a laser or chemicals such as ferric chloride. Depending on the type of injury, several parameters can be analyzed such as occlusion time, platelet deposition, and thrombus size. Although the carotid artery is not easily accessible, its large size enables also blood flow measurements (e.g., using ultrasonic probes).

IVM of carotid artery ligation and ferric chloride ($FeCl_3$) injury are two popular experimental approaches used in assessing arterial thrombosis. Carotid artery ligation involves mechanical damage caused by tying a suture around the artery for a given time. The resulting loss of the endothelial cell layer at the site of injury[1] initiates platelet tethering within the first minutes after endothelial denudation. Platelet adhesion is mostly firm and irreversible and adherent platelets recruit additional platelets from the

received
May 2, 2023
accepted after revision
July 4, 2023

Georg Thieme Verlag KG,
Rüdigerstraße 14,
70469 Stuttgart, Germany

DOI https://doi.org/10.1055/a-2118-2932.
ISSN 0720-9355.

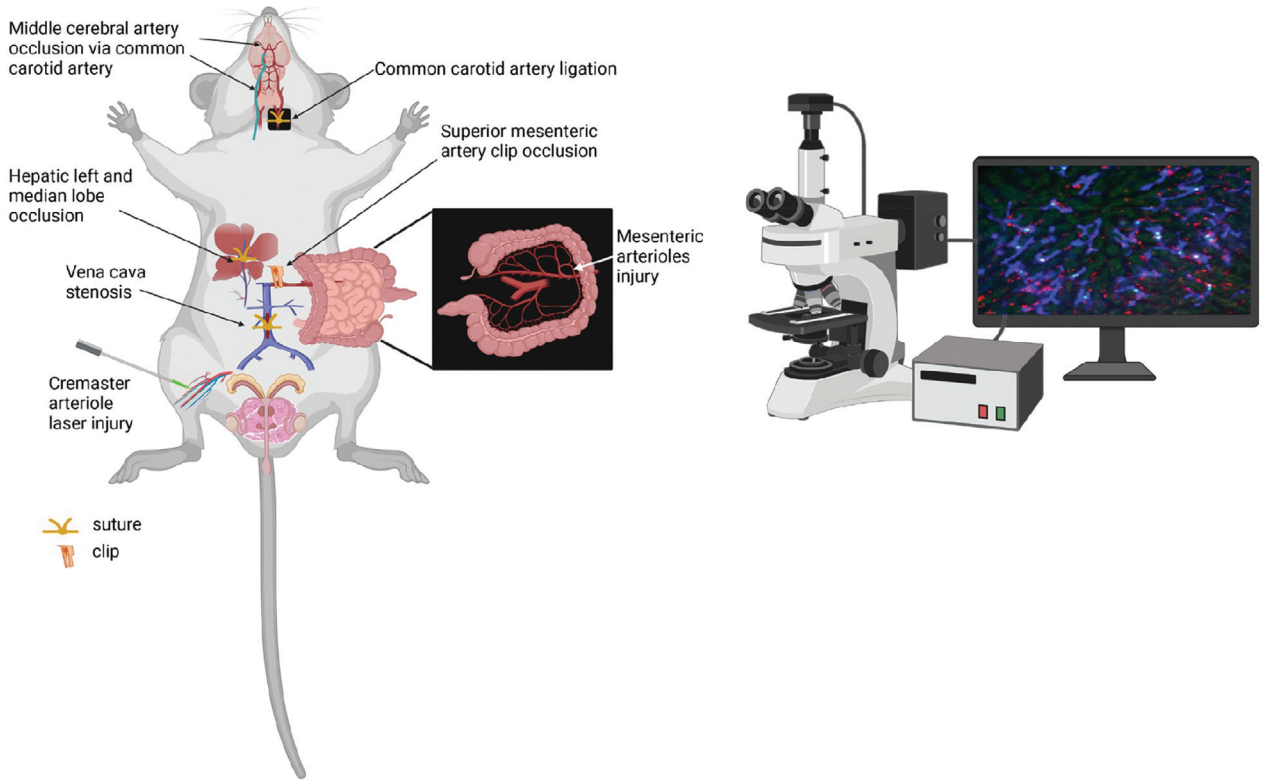

Fig. 1 Overview of thrombosis models that can be studied using intravital microscopy. Depicted are common vascular beds and injuries: middle cerebral artery occlusion, common carotid artery ligation, liver ischemia reperfusion, vena cava stenosis, cremaster arteriole laser injury, and mesenteric arteries/arterioles injury (created with BioRender.com). [rerif]

Table 1 Summary of thrombosis models suitable for intravital microscopy that are being discussed in this article.

Technique/vascular bed	Advantages	Disadvantages
Carotid artery injury (ligation, $FeCl_3$-induced injury)	- Well characterized (GPVI, GPIb, TF dependent) - Occlusion time, platelet deposition, thrombus size, and blood flow can be measured	- Risk of movement artifacts - Artificial injuries - $FeCl_3$ concentration and incubation time needs to be titrated
Atherosclerotic plaque rupture (*Apoe*$^{-/-}$ mice, high fat diet)	- Better resembles the physiologic situation - Thrombus formation upon plaque rupture can be assessed in real time	- Less well studied than other models
(Transient) middle cerebral artery occlusion	- Well established (GPVI, GPIb-dependent) - Platelets and leukocyte recruitment can be visualized	- Advanced surgery skills necessary
Mesenteric arteries/arterioles ($FeCl_3$, laser injury, ischemia)	- Well established - Good accessibility of the vessels - Thrombus formation can be followed in real time	- $FeCl_3$ concentration and incubation time needs to be titrated - Fat deposition influences extent of injury
Cremaster arteriole laser injury	- Platelet and fibrin deposition can be followed in real time	- Laser ablation setup necessary - Variability of the injury
Inferior vena cava stenosis	- Physiologic stimulus (blood stasis)	- Thrombus formation takes days
Liver thrombosis (infection)	- Thrombus formation can be followed in real time after infection	- Stable liver preparation can be difficult to obtain, (especially over time)
Liver ischemia reperfusion injury	- To some degree models pathophysiologic condition after transplantation - Insights potentially applicable to other ischemic diseases	

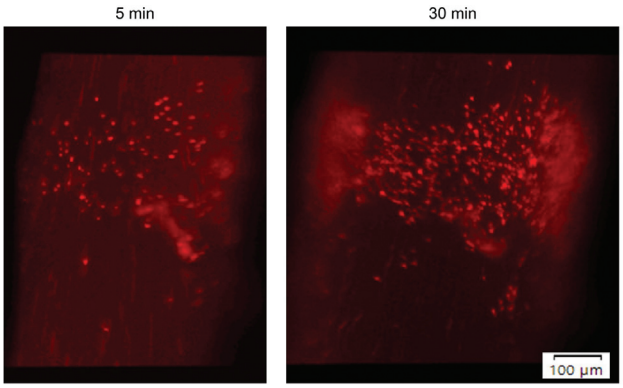

Fig. 2 Intravital imaging of the carotid artery thrombosis model. Mice were anesthetized and a polyethylene catheter was implanted in the jugular vein. Rhodamine B *ex vivo*–stained platelets were infused. The left common carotid artery was dissected and ligated with a polypropylene suture for 5 minutes. Platelets were visualized by *in vivo* epifluorescence high-speed video microscopy 5 or 30 min after vascular injury.

circulation, thus contributing to the growing thrombus. This dynamic process depends on glycoprotein VI (GPVI), the major platelet collagen receptor and GPIbα which mediates platelet collagen binding indirectly, through von Willebrand factor (VWF).[1] Tissue factor microparticles are considered to contribute to thrombus formation, too.[2] At the sites of vascular injury, plasma VWF promotes platelet adhesion to the extracellular matrix, and platelet aggregation, in particular as wall shear rates increase.[3,4] Common readouts are platelet deposition (platelet count) and thrombus growth (area covered) over time (►Fig. 2).

Ferric chloride injury involves the topical application of ferric chloride solution to the adventitial surface of the carotid artery. This causes endothelial cell damage and exposure of the subendothelial matrix resulting in platelet activation, aggregation, and thrombus formation. The application of $FeCl_3$ to the vessel wall causes major oxidative stress and generation of free radicals leading to lipid oxidation, destruction of endothelial cells, and subsequent thrombus formation. More specifically, $FeCl_3$ crosses the endothelium in small vesicles by an endocytic–exocytic pathway, thereby causing complete endothelial denudation.[5] Microparticles containing ferric iron and tissue factor, surrounded by a tissue factor-rich endothelial cell membrane bilayer, are also present in the thrombus environment[6] and are in direct contact with fibrin fibers already 2 minutes after injury. Apart from the direct effect of $FeCl_3$ on the endothelial cell layer, it also caused erythrocyte hemolysis and hemoglobin oxidation *ex vivo* which promoted endothelial denudation.[7] However, this could not be reproduced *in vivo*.[6] Both thrombin generation and platelets were shown to play an important role in the $FeCl_3$ model.[6] And while there was some debate over the role of the collagen receptor GPVI,[6,8] using genetic knockout mice as well as blocking antibodies, it was shown that GPVI and GPIb contribute to thrombus formation in $FeCl_3$-induced injury models *in vivo*.[1,9] Typically, time to vessel occlusion and thrombus size are quantified and analyzed. Several factors need to be standardized in this model such as the concentration of $FeCl_3$ in the solution (usually between 5 and 20%), the application (soaked filter paper or drop), as well as the incubation time (2–5 minutes). High $FeCl_3$ concentrations can result in vessel opacification hampering the thrombus visualization.

Both techniques have their advantages and limitations. Carotid artery ligation is a more controlled method in terms of thrombus initiation and is easy to standardize between animals. Ferric chloride injury on the other hand is more difficult to standardize. Despite carefully controlling the size and position of the $FeCl_3$-soaked filter paper, thrombus formation can vary[5] with some vessels showing partial occlusion while others exhibiting exuberant thrombus formation that extends beyond the limits of the filter paper.

One drawback of both models presented is that neither mechanical nor ferric iron-induced injuries are (patho)physiologic injuries. In addition, in both models, the injury is caused to healthy blood vessels, which does not mimic the human disease, as the main reason for arterial thrombosis is atherosclerotic plaque rupture. To overcome this issue, Kuijpers and colleagues developed a model in *Apoe*$^{-/-}$ mice fed with high fat diet to investigate thrombus formation after atherosclerotic plaque rupture using an ultrasound probe.[10,11] In this model, atherosclerotic arteries showed loose thrombi consisting of platelets, erythrocytes, collagen, and fibrin. Rupture was induced by ultrasound application and the following platelet adhesion and thrombus formation was analyzed using intravital fluorescence microscopy.

Studying Thromboinflammation Using (Transient) Middle Cerebral Artery Occlusion Models

Ischemic stroke in humans is commonly caused by blockade of the middle cerebral artery (MCA). Therefore, MCA occlusion (MCAO) in rodents is frequently used to model ischemic stroke and to study its pathophysiology and potential treatments. In the late 1980s, Koizumi *et al.* and Longa *et al.* described the first MCAO models in rats that were performed without craniotomy.[12,13] Animals were anesthetized and carotid arteries were dissected and the common carotid artery (CCA) was located next to the trachea. Ligatures were tied around the proximal CCA and the external carotid artery (ECA). A tourniquet was loosely tied around the distal CCA. A vessel clip was used to cut the blood flow at the distal CCA. Next, an incision was made between the ligature at the proximal CCA and the vessel clip at the distal CCA. A (silicon-tipped) filament was inserted into the CCA, the vessel clip removed, and the filament advanced into the internal carotid artery and further intracranially to occlude the MCA at its origin.[14] The end of the filament was secured by tightening the tourniquet and left in place for 30 to 120 minutes to induce transient ischemia and allow subsequent reperfusion. Alternatively, the filament stayed in place for 24 hours to cause permanent occlusion.[15] The filament-based transient (t) MCAO model is now the most common technique to model ischemic stroke in rodents and causes neuronal cell death, glial cell activation, and blood brain barrier damage.[16] However, significant practice is needed to reproduce comparable infarct volumes. Typical outcome measures after (t)MCAO

include infarct volume, histology/immune fluorescence staining, and scoring of the neurological and motor function. To assess infarct size, brain sections are stained using triphenyltetrazolium chloride (TTC) and the ischemic (whitish) areas quantified using image analysis software. The Bederson test is commonly used to assess neurologic functions,[17] whereas the string or grip test allows to score motor function.[18]

Restoring blood flow in acute stroke (e.g., through thrombolysis or mechanical thrombectomy) remains the main treatment goal in the clinic. However, especially when reperfusion is achieved too late, further damage and infarct growth is frequently observed—a phenomenon termed *reperfusion injury (RI)*. During RI, reactive oxygen species (ROS) are generated which directly damage cells and spark inflammation (e.g., through the release of damage-associated molecular patterns [DAMPs])[19] that leads to the upregulation of cell adhesion molecules and leukocyte recruitment. In addition, platelets adhere to and become activated at the site of vascular damage, thereby increasing the risk of secondary thrombotic events.[20] Thus, both thrombotic and inflammatory pathways are active following brain ischemia. The interplay and amplification between these two pathways has been termed *thromboinflammation*.[21] Using the tMCAO model in combination with genetically modified animals has allowed to unravel key players in thromboinflammation after stroke such as platelet receptors GPIb and GPVI[22] as well as soluble factors released from platelet alpha and dense granules.[23,24]

Dong and colleagues assessed the impact of intravenous administration of Resolvin D2 (RvD2)-loaded nanovesicles[25] on inflammation after ischemic stroke using the tMCAO model. Nanovesicles were labeled with the lipid dye DiR (1,1′-dioctadecyl-3, 3, 3′, 3′-tetramethylindotricarbocyanine iodide) which emits light in the near-infrared spectrum. Ex vivo analysis of brain sections using an IVIS imaging system at different time points post reperfusion showed that the nanovesicles specifically accumulated in the ischemic brain hemisphere.

To study the mechanism on a cellular level, the authors set up intravital microscopy of the mouse brain using a cranial window. Mice were anesthetized and a dorsal midline incision was made to expose the skull. A high-speed drill was used to remove a circular area of the skull bone above the right brain hemisphere. A glass cover slip was placed on the top of the dura mater and super glue was applied to secure it in place.[25,26] Lastly, a bar was mounted on the head to later attach the mouse to the microscope imaging stage. After surgery, mice were allowed to recover before the tMCAO procedure. Seven days after implantation of the cranial window, mice were imaged using an intravital microscope (e.g., laser scanning confocal microscope or multiphoton microscope if deeper tissue penetration is desired). DiR-labeled nanovesicles were injected 1 hour after reperfusion, followed by BSA-Cy5 and Ly-6G-Alexa Fluor 488 antibody to label the vessel lumen and neutrophils, respectively. Using this setup, the authors visualized the binding of nanovesicles to inflamed brain vasculature in real time and also observed the reduced recruitment of neutrophils after treatment with RvD2-loaded nanovesicles.[25]

In another study, Desilles and colleagues performed partial dura-sparing craniotomy in rats followed by 60 minutes of tMCAO. Intravital fluorescence microscopy was used to visualize platelets and leukocytes as well as fibrinogen during MCAO and after recanalization in pial vessels.[27] During MCAO, they observed fibrin(ogen) deposition in postcapillaries colocalizing with leukocyte and platelet accumulation. These microthrombi then caused full vessel occlusion in one or more vessels per field of view. Platelets and leukocytes remained attached even after reperfusion. On the other hand, Göb *et al.* used light sheet fluorescence microscopy after tMCAO and found that tissue damage peaked at 8 hours after reperfusion, while thrombi were observed only at later time points, thereby suggesting that thrombosis was not the driving force of secondary infarct growth after stroke.[28]

Ishikawa *et al.* investigated the role of CD40 and CD40L in cerebromicrovascular dysfunction and tissue damage following transient MCAO using a cranial window and intravital microscopy. They performed a craniotomy 1 mm posterior from the bregma and 4 mm lateral from the midline leaving the dura mater intact. A cover glass was placed over the exposed brain tissue. Both CD40- and CD40L-deficient mice showed reduced infarct volumes after tMCAO compared to control mice after 1 hour of MCAO followed by 4 hours of reperfusion.[29] Platelets were isolated from donor mice and labeled with carboxyfluorescein diacetate succinimidyl ester (CFSE). 10^8-labeled platelets were infused into recipient mice over 5 minutes via the femoral vein. Rhodamine 6G was used to label endogenous leukocytes. Using intravital microscopy they found that both platelet and leukocyte adhesion was reduced in CD40/CD40L-deficient animals.

These studies show that the tMCAO model combined with intravital microscopy, transgenic mice, and appropriate labeling allows to obtain insight into the pathomechanism of ischemic stroke and RI on the cellular level.

Mesentery

Due to their easy access, mesenteric vessels are very well suited for intravital microscopy and different ways to induce thrombus formation exist. One common method uses application of $FeCl_3$ to the mesenteric arterioles (for a detailed protocol see Kuijpers and Heemskerk[11] and Bonnard and Hagemeyer[30]). Briefly, after anesthetizing the mice, staining or stained cells are injected either via the tail or the jugular vein and the intestine is carefully exposed. Injury is caused by placing a $FeCl_3$-soaked filter paper on the arteriole of interest. In this model, thrombus growth was shown to depend on platelet $P2Y_{12}$ ADP receptor,[31] GPVI,[32] and VWF.[33] The method is rather simple, yet many variables need to be optimized. The reproducibility is affected by the size of the vessels, which often vary even among mice of the same age. Vessel-associated fat may compromise reproducibility, as it affects the extent of the injury[30] and therefore the use of younger animals is preferred. A second approach which is easier to standardize is the laser injury model; however, the thrombotic effect is less pronounced compared to chemical injury.[33]

Apart from chemical or laser damage in mesenteric arterioles, there is the model of *in vivo* gut ischemia/reperfusion (I/R) injury which is often investigated by inflicting damage to the superior mesenteric artery—the most important vessel for blood supply to the colon in rodents.[34] This model is used to mimic I/R-induced intestinal injury often occurring in bowel ischemia, abdominal aortic aneurism repair, and abdominal compartment syndrome.[35] Intestinal I/R starts with ischemia which results in hypoxia and malnutrition, leading to energy metabolism disorders.[36] Lack of ATP impacts a range of ATP-consuming processes such as cation pumps and F-actin polymerization. Consequently, endothelial and epithelial barriers break down. Restoration of blood flow, however, results in greater tissue injury[37] due to ROS production and ischemia RI.

Acute mesenteric infarction is characterized by a disrupted gut barrier and dysregulation of the host immune response.[38,39] Bacteria or bacterial products leak through the compromised barrier from the gut lumen to the circulation and promote leukocyte adhesion on the endothelial cells of the mesenteric venules.[40,41] The process is more complex than $FeCl_3$-induced injury as it is based on arterial occlusion. After identification of the superior mesenteric artery, it is carefully occluded with a small vascular clamp. It is important to keep the exposed intestine moist and to avoid trauma by touching it, otherwise this would lead to unintended platelet and leukocyte adhesion that is not caused by the blood stasis. The time of occlusion as well as the time of reperfusion can be varied and afterwards the mesenteric venules are observed by microscopy and platelet and leukocyte rolling and adhesion can be quantified (►Fig. 3).

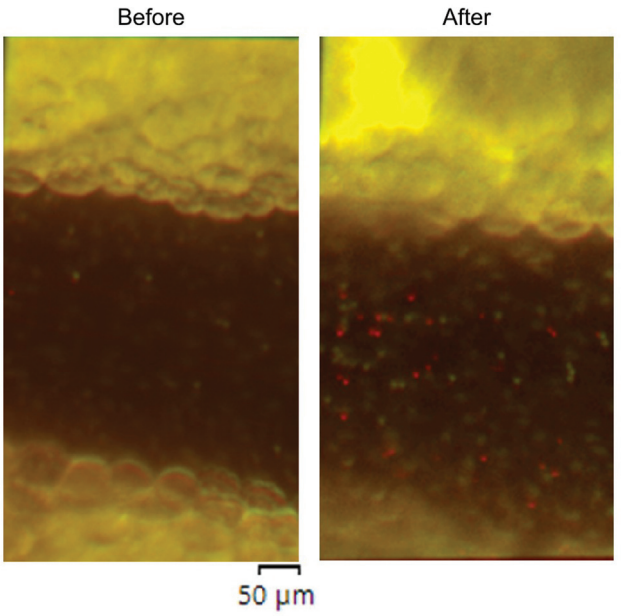

Fig. 3 Intravital imaging of mesenteric ischemia reperfusion injury. Mice were anesthetized and a polyethylene catheter was implanted in the jugular vein. Rhodamine B *ex vivo*–stained platelets were infused. Following a midline laparotomy, the superior mesenteric artery was identified and occluded with a small vascular clamp. After 60 minutes of ischemia, reperfusion was allowed. Before and immediately after ischemia-reperfusion, the entire small intestine was carefully taken out of the abdomen. Platelets and leukocytes (stained with acridine orange infusion via the catheter shortly before imaging) were visualized in situ by *in vivo* epifluorescence high-speed video microscopy in the mesenterial venules before and after the vascular injury.

Cremaster Arteriole Laser Injury Model

By combining laser-induced injury and state-of-the-art imaging techniques, it is possible to investigate the kinetics and molecular mechanisms of *in vivo* thrombus formation. Injury is achieved by using a focused laser pulse to the vessel wall of an arteriole inside the cremaster muscle. With this technique, it is possible to control the place and time of thrombus formation *in vivo*. The accumulation of the main components of thrombi—platelets and fibrin—can be visualized easily by using fluorophore-conjugated antibodies combined with intravital microscopy. Recent advances in this technique also allow the analysis of the thrombi architecture, signaling pathways, calcium mobilization, blood flow velocity around the thrombus and even the formation of multiple thrombi in close distance to each other.[42,43]

To perform this model, mice are anesthetized and a catheter is placed into the jugular vein for application of additional anesthesia and fluorophore-conjugated antibodies or labelled cells.[44] Externalization of the testis and anus as well as removal of excessive tissue and fat allows free access to the cremaster muscle. Afterward, the cremaster muscle needs to be expanded to a cover-slip and fixed with a pin to the imaging tray.[45] Visualization of platelets, fibrin, and other factors can be achieved either by the administration of fluorophore-conjugated antibodies or by intravenous injection of exogenous labelled platelets.[46]

The injury is usually induced using a pulsed nitrogen laser at 440 nm.[42] The power of the laser should be adjusted based on the desired size of the injury, the diameter of the arteriole, the thickness of the muscle, and the size of the intended thrombus. Thrombus-forming injuries to the vessel wall can already be induced with one to two pulses,[46,47] but depending on the laser power, also up to 10 pulses, could be necessary.[48] The laser is focused on the luminal surface of the arterioles.[49] Some research groups perform their laser-induced injury by using repeated, very short laser pulses (3–5 ns) with a distance of 500 nm between each in a two-by-two pattern. With a total of 24 pulses/injuries, this method is gentle and no subendothelial collagen is exposed during the vascular injury. The injury is achieved by laser-mediated activation of the endothelium.[42,50] The groups of Atkinson *et al.* and Dubois *et al.* showed that there was no difference between a single injury per mouse versus multiple upstream injuries.[46,47]

Shortly after laser-induced injury, thrombus formation can be observed using a bright-field microscope or fluorescence microscope based on the aim of the experiment. Usually, the whole procedure is performed in an intravital microscopic setting. Basic measurements include the increase in fluorescence signal by labelled platelets and fibrin at the site of the injury. Also, factors such as thrombin and tissue factor can be labelled and their impact on thrombus

formation observed.[49] By measuring the thrombus formation over time, a thorough understanding of the kinetics under different conditions (based on the model) can be achieved. For instance, labeling platelets, fibrin and activated $\alpha_{IIb}\beta_3$ integrin can give information on the kinetics of $\alpha_{IIb}\beta_3$ integrin activation as well as the size and stability of the thrombi.[51] To reduce concurrent activation, $\alpha_{IIb}\beta_3$ integrin inhibitors such as eptifibatide can be used.[47] To investigate the external environment of the thrombus like the velocity of red blood cells, externally labelled red blood cells can be injected and their flow around the thrombus measured with intravital microscopy and analyzed using image analysis software such as Slidebook, Volocity, or Imaris.[50]

For the analysis of thrombus formation kinetics and the influence of emboli on downstream thrombi, a standard bright-field microscope should be sufficient. Also, the diameter of the vessel up- and downstream to the injury can be assessed.[50] For a more in-depth analysis of the thrombi components, the kinetics of platelet and fibrin binding (taking the median fluorescence intensity and by co-localization of the platelet and fibrin signal) or the influence of tissue factor, thrombin, or $\alpha_{IIb}\beta_3$ integrin, a multichannel fluorescence microscope is essential.[52,53] The architecture of thrombi can later be inspected using confocal microscopy on thin sections of the microvasculature or thrombi.[43,46] With intravital microscopy, it is also possible to record videos of the thrombus formation.

One limitation of this technique is the high variability between single injuries. The degree of injury is highly dependent on the vessel itself, the thickness of the muscle, and the laser power.[42]

Venous Thrombosis

A very well characterized model to study venous thrombosis *in vivo* is the stenosis model of the inferior vena cava (IVC). This model mimics deep vein thrombosis (DVT), occurring most frequently in lower limbs which could result in pulmonary embolism if the thrombus detaches from its initial location and occludes the vasculature of the lungs. These two diseases together are some of the most common vascular disease worldwide.[54] DVT is usually caused by cancer, trauma, or blood stasis,[55] and once the thrombus gets detached from its initial location and reaches the lungs, it leads to pulmonary embolism. In the *in vivo* model of DVT, thrombosis can be induced either by stenosis, ferric chloride, or laser injury.[56]

Although the application of ferric chloride on the IVC can chemically induce thrombosis,[57] thrombus formation is caused by nonphysiologic processes, which are not representative of the human disease, where thrombosis is usually initiated by blood stasis.[58] Nevertheless, ferric chloride induces a rapid leukocyte- and platelet-rich thrombus formation already 1 minute after application.[57] Such fast response is different from human disease progression, but enables the quick experimental observation of thrombus growth.[57] DVT in the IVC can also be induced by stenosis or complete occlusion models (for protocols see Payne and Brill[59] and Wrobleski *et al.*[60]).

During the vena cava stenosis model, a space holder is secured on the vessel with a permanent narrowing ligature, restricting the flow. Removal of the wire leads to flow restriction but not occlusion, mimicking human disease progression. The thrombus growth can be observed periodically under the microscope, after infusion of the appropriate fluorescently labeled cells, dyes, or antibodies. However, the *in vivo* observation time is limited to a certain timeframe during thrombus formation since extensive imaging sessions might increase the risk of nonphysiologic reactions. At the end of the experiment, the occlusive thrombus can be characterization *ex vivo*.

The *ex vivo* thrombus analysis proved that inflammatory processes and DVT are closely linked. Leukocyte adhesion occurs as early as 1 hour after IVC stenosis and increases dynamically on the thrombosed vein wall with tumor necrosis factor-α playing a pivotal role in neutrophil extravasation. During thrombus maturation (day 6), neutrophils are accompanied by monocytes and lymphocytes.[61] An *in vivo* model with 80% flow restriction leads to the formation of small thrombi after 6 to 12 hours with occlusion happening between 24 and 48 hours in 60% of the mice.[62]

The observation of early thrombus formation during murine DVT with intravital microscopy (e.g., 6 hours after stenosis) showed that similarly with the *ex vivo* analysis, the process is dominated by leukocyte adhesion.[62] The exposure of adhesive molecules such as P-selectin and VWF factor proves that the activation of the endothelium is a response to depressed blood flow.[62] The inflammatory response leads to activation of the coagulation cascade initiated by leukocyte-derived tissue factor, which subsequently results in fibrin formation. Neutrophils promote the growing thrombus further by releasing neutrophil extracellular traps (NETs) 3 hours after flow restriction. In contrast to arterial thrombosis, where platelets dominated the thrombus growth within minutes of stenosis, in this model, platelets are adhering either on the activated endothelium or on leukocytes, but are outnumbered by the inflammatory cells, which also proceed this process. Yet, the interaction between platelets and neutrophils is critical for thrombus development. Inhibition of platelet G protein–coupled receptors and immunoreceptor tyrosine-based activation motif signaling results in reduced platelet adhesion to the inflamed vascular wall, impaired neutrophil activation, and thus reduced stenosis-induced thrombus formation.[63]

The vena cava stenosis model has several limitations. To better mimic the human disease, the thrombus formation should occur only due to the flow restriction and not based on endothelial denudation. Therefore, all mice that show bleeding events during the stenosis should be excluded from the study. Also, the thrombus occurrence often varies or is completely absent.[62] The vascular anatomy in mice is highly variable. There are different numbers of lateral and dorsal branches on the vena cava, even among mice of the same strain, providing alternative circulatory paths for the venous flow. It has been shown that the number of lateral branches is

often the reason for the absence of thrombus formation in this model.[64,65] Interestingly, the thrombus occurrence does not depend on the flow in these branches, rather on the distance of the confluent side branch from the stenosis suture. Ligation of these branches does not impact the thrombus size or the variability of thrombus formation[66] and reduces the variability of the model but induces endothelial injury.[67] In order to visualize the early stage of thrombus formation in the completely occluded IVC *in vivo*, the side branches need to be intact so that the flow persists.

Liver Thrombosis Models

Infection-Mediated Liver Thrombosis

Thrombosis is a common complication of systemic infection and can be associated with multiorgan damage. Inflammation following infection activates platelets, which may accompany endothelial damage and thrombus development. This process is frequently referred to as *immunothrombosis*.[68]

Here, we highlight different infection-induced thrombosis models focusing our attention on thrombi formation in the liver and the techniques that have been used, so far, to study this phenomenon. Depending on the model, liver thrombosis can be induced following the injection of a single antigen such as LPS and alpha toxin, or entire bacteria in mice.[69]

Studies by Hitchcock *et al.* as well as Beristain-Covarrubias *et al.* focused on inflammation-driven thrombosis induced by *Salmonella* Typhimurium (STm) infection of mice.[70,71] By means of tissue staining and flow cytometric analysis of liver tissue, they observed a novel pathway of thrombosis. After infection, inflammation directly induces thrombosis by upregulating podoplanin on monocytes/macrophages resulting in CLEC-2-mediated platelet activation.[70] Immunohistological staining also showed that thrombus formation in the liver was occurring 7 days after infection and persisted even after the infection was resolved. Another study focusing on STm infection showed that thrombosis can have different kinetics. By immunohistological and immunofluorescent staining, they characterized both liver and spleen and observed that thrombi formation can occur sequentially in multiple tissues, opening the doors for a possible targeted therapeutic treatment.[71]

During staphylococcal sepsis, patients develop microvascular thrombosis with a tendency toward systemic bleeding, possibly caused by abnormalities in platelet function.[72–74] Intravenous injection of alpha toxin has been used to establish a mouse model of staphylococcal sepsis.[75–77] Surewaard and colleagues took advantage of spinning disk intravital microscopy to investigate the role of *Staphylococcus aureus* infection on the microvasculature.[77] This powerful technique allows to study the interactions of microbes with different host cells, such as immune cells and platelets in real time. Mice were anesthetized and a tail vein catheter was inserted to inject fluorescent antibodies and to maintain anesthesia. An incision is made along the midline of the abdomen to expose underlying organs. The mouse is placed on its right side onto the microscope stage and one liver lobe is carefully guided onto the microscope cover glass.[78] To model acute sepsis, alpha-toxin, culture supernatants, or live bacteria, were injected intravenously and platelet aggregation and bacteria were observed and analyzed using image analysis software to quantify the amount of platelet aggregation and thrombi formation (►Fig. 4). The approach used in this study demonstrated that intravenous alpha-toxin injection results in rapid platelet aggregation with subsequent micro-thrombi formation in the microcirculation. These aggregates accumulated in the liver sinusoids and kidney glomeruli causing multiorgan dysfunction. Furthermore, they observed that treatment with an alpha-toxin neutralizing antibody prevented platelet aggregation and subsequent damage, without affecting platelet contribution to eradicating *S. aureus* infection.[77]

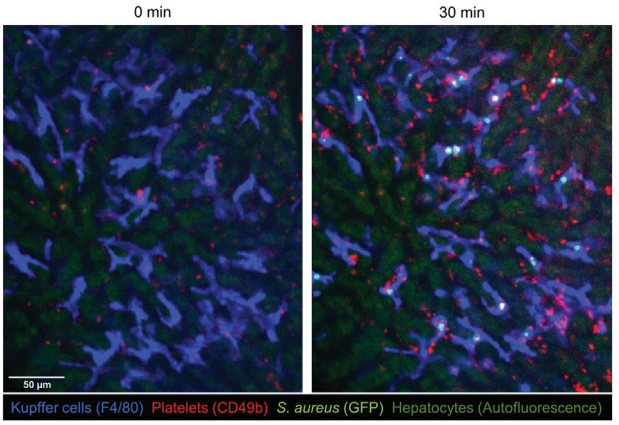

Fig. 4 Intravital imaging of sepsis-associated liver thrombosis. Mice were anesthetized and a jugular vein catheter was inserted to inject fluorescent antibodies and maintain anesthesia. Image acquisition was performed using an inverted spinning disk confocal microscope. Kupffer cells and platelets were visualized using fluorescently labeled antibodies against F4/80 and CD49b, respectively. Mice were intravenously injected with 5×10^7 colony-forming units (CFUs) of GFP-expressing *Staphylococcus aureus*. Shown are images before and 30 min post *S. aureus* injection.

Hepatic Ischemia Reperfusion Injury

Liver resection and liver transplantation sometimes represent the only available treatment for patients with liver disease.[79] Hepatic I/R injury is a common complication of these procedures and is one of the primary causes of early organ dysfunction and failure after the procedure. I/R injury is a pathological process involving ischemia-mediated cellular damage followed by a paradoxical exacerbation upon reperfusion of the liver.[80,81] This phenomenon engages many different cell types and several signaling pathways. During the first phase, the ischemic insult exposes hepatic cells to oxygen deprivation, pH changes, and ATP depletion. This condition forces the cells to rely on anaerobic metabolism for energy production.[82] Consequently, ROS production is enhanced, leading to organelle damage, hepatic cell injury, and death.[83] The following reperfusion causes a profound inflammation which aggravated hepatocellular damage.[84–86] Even though I/R injury has been widely investigated, its

mechanisms remain largely unclear. In this context, animal models are valuable tools for understanding the physiopathology of hepatic I/R injury, clarifying the molecular mechanisms involved and discovering novel therapeutic targets and drugs. DAMPs released from dead cells after I/R injury activate Kupffer cells leading to the release of chemokines and cytokines and result in the recruitment of immune cells such as circulating monocytes, neutrophils, and T cells to promote hepatocellular injury.[87] Zhang *et al.* studying a mouse model of I/R injury showed by flow cytometry, that Kupffer cells were a major source of CCL2, which attracts $CCR2^+$ neutrophils into the ischemia–reperfusion-stressed liver.[88] Kupffer cells also produce CXCL1, CXCL2, and CXCL8 upon liver injury.[89,90] A study by de Oliveira *et al.* used confocal intravital microscopy to image neutrophil migration in the liver of Lysm-eGFP mice subjected to I/R injury.[91] These reporter mice express the green fluorescent protein (eGFP) mainly in neutrophils.[92] Mice are anesthetized, a midline laparotomy is performed, and mice are subjected to I/R by occluding the pedicle of the left and median lobes of the liver, which contains the bile duct, hepatic artery, and portal vein, using an atraumatic clamp. After 60 minutes of ischemia, the clamp is removed and reperfusion is allowed. Neutrophil accumulation in the liver is observed using intravital microscopy of GFP-bright cells, excluding low–GFP-expressing mononuclear cells.[93] After different reperfusion times, the mice are anesthetized and the liver is carefully exposed. Sytox orange is injected intravenously to stain DNA and show necrotic cells. Imaging analysis software is used to analyze neutrophil count, location, and migration distance. Time points between 1 to 48 hours after reperfusion were chosen for examination. They observed that treating mice with reparixin, a CXCR1/2 receptor antagonist, significantly decreased neutrophil activation and infiltration in the liver. Additionally, reparixin was able to reduce the reperfusion-associated tissue damage, suggesting that the blockage of CXCR1/2 could be a possible therapy for patients undergoing liver surgery.[91]

The first evidence of the involvement of platelets in the development of I/R-induced hepatic injury was obtained by Cywes *et al.* who showed platelet infiltration in the perfused rat liver using electron microscopy and in the human liver using immunohistochemistry.[94–96] Later, Khandoga *et al.*, using intravital microscopy, observed that hepatic I/R induced both transient interaction and permanent adhesion of platelets to the post-ischemic liver sinusoids. The number of these contacts during early reperfusion depended on ischemia time.[97] P-selectin is a major adhesion molecule involved in platelet and leukocyte adherence to the endothelium.[98] Mice deficient for P-selectin display reduced platelet and neutrophil accumulation, a decrease in post-ischemic liver injury, and improved survival following warm ischemia.[96,99] Treatment with the selective PAR-4 antagonist TcY-NH2 attenuated I/R-induced platelet and $CD4^+$ T-cell recruitment, improved sinusoidal perfusion, and reduced apoptotic injury.[100] Also, antifibrinogen antibody administration inhibited platelet adhesion and decreased short-term liver injury in a mouse model of liver I/R injury.[101] In response to I/R, platelets become activated and release factors that promote liver injury as well as hepatic regeneration such as platelet-activating factor (PAF), cytokines, nitric oxide (NO), transforming growth factor-β (TGF-β), and serotonin. PAF, also produced by Kupffer cells and liver sinusoidal endothelial cells, acts on neutrophils boosting ROS generation, further contributing to the amplification of the neutrophil response.[102] NO produced by platelets combined with oxygen-free radical formation upon reoxygenation of the ischemic liver can lead to the production of peroxynitrite, which can support programmed cell death in endothelial cells.[103–105] Platelet-derived serotonin has been exhibited to promote hepatocellular proliferation and tissue repair, also in the context of hepatic ischemia in mice.[106,107] Nocito *et al.* assessed the impact of platelets in hepatic I/R injury using mouse models of impaired platelet function and platelet depletion via clopidogrel administration and injection of anti-CD41 antibody, respectively. Partial hepatic ischemia was induced for 60 minutes, and different time points of reperfusion were evaluated. Interestingly, they observed that impairment of platelet function and platelet depletion had no direct effect on I/R injury, while liver regeneration and repair were significantly impaired in platelet-depleted animals.[107]

Another study conducted by Zhang *et al.* focused on the possible interplay between neutrophils and platelets in liver I/R injury.[108] In this study, I/R was performed by occluding the left and median liver lobes with a microvascular clamp for 90 minutes, followed by reperfusion times of 6, 12, and 24 hours. Interestingly, flow cytometric analysis showed that mice subjected to liver I/R displayed systemic platelet activation and increased platelet-neutrophil aggregates. Liver I/R resulted also in injury in distant organs such as kidney and lung with increased NETs and platelet-rich microthrombi formation. Blocking NETs by DNase treatment decreased organ damage as well as thrombi formation in mice. Moreover, using a platelet-specific TLR4 KO mouse model, they observed that following liver I/R, mice had reduced distant organ injury with decreased circulating platelet activation and platelet-neutrophil aggregates.[108]

Conclusion/Outlook

Here, we showcase how intravital microscopy allows to visualize platelet and immune cell recruitment at sites of thrombus formation in different vascular beds with distinct physiological properties. The diameter and blood flow rates of each vessel determine the respective wall shear rates. While the shear rate in the healthy mouse carotid artery averages 1,800 to 4,000/s, it is lower in the mesenteric arteries (1,200–1,700/s) and even lower in the cremaster arteriole (700–1,000/s).[109] To visualize fast moving cells such as platelets in the blood stream, high imaging speeds are needed and nowadays resonant scanners are the solution offered for most confocal and two-photon microscope systems. These devices contain mirrors that oscillate at a resonant frequency of 8 kHz or higher, resulting in scanning speeds of more than 30 frames per second for images with

512 pixels in height (=lines to scan). Nevertheless, good results can also be obtained using epifluorescence microscope systems equipped with high-speed cameras which are more than sufficient for imaging e.g. the mesenteric arteries. Thus, good intravital setups do not have to be very expensive. More important is a stable preparation of the vessel/organ to be visualized since inherent movements from heartbeat, breathing, or gut motility can severely impair imaging quality. This is in fact one of the challenges when setting up intravital microscopy of the carotid artery since vessel pulsation is difficult to control. One solution is to acquire only images that originate from the same focal plane during the (mostly) regular movement. Inherent movement and difficult accessibility have for a long time hampered intravital imaging of the beating heart. That is why we did not include a section on myocardial infarction in this review. However, recent advances in imaging the beating mouse heart are promising.[110,111] Another trend is the increasing use of artificial intelligence to help the user with image acquisition and analysis. For example, using a trained convolutional neural network, Mahmoud and colleagues were able to analyze microvascular flow in images obtained from IVM. First, they used a vessel segmentation algorithm to identify the vasculature and in a second step the trained neural network analyzed the three-dimensional imaging data to determine whether the vessel showed blood flow or not.[112] We expect advances in the development of imaging hardware and analysis software tools to further increase the productivity and accessibility of imaging systems and that these systems will soon become standard technology in most thrombosis and hemostasis research laboratories.

Conflict of Interest

The authors declare that they have no conflict of interest.

Acknowledgements

K.K. is supported by the German Center for Cardiovascular Research (DZHK) "Promotion of women scientists" Excellence Program and is a member of Young DZHK. M.C. and C.D. are supported by the German Research Foundation (DFG) project number 318346496, SFB1292/2 TP08.

References

1 Massberg S, Gawaz M, Grüner S, et al. A crucial role of glycoprotein VI for platelet recruitment to the injured arterial wall in vivo. J Exp Med 2003;197(01):41–49
2 Reinhardt C, von Brühl ML, Manukyan D, et al. Protein disulfide isomerase acts as an injury response signal that enhances fibrin generation via tissue factor activation. J Clin Invest 2008;118 (03):1110–1122
3 Savage B, Almus-Jacobs F, Ruggeri ZM. Specific synergy of multiple substrate-receptor interactions in platelet thrombus formation under flow. Cell 1998;94(05):657–666
4 Jäckel S, Kiouptsi K, Lillich M, et al. Gut microbiota regulate hepatic von Willebrand factor synthesis and arterial thrombus formation via Toll-like receptor-2. Blood 2017;130(04):542–553
5 Tseng MT, Dozier A, Haribabu B, Graham UM. Transendothelial migration of ferric ion in FeCl3 injured murine common carotid artery. Thromb Res 2006;118(02):275–280
6 Eckly A, Hechler B, Freund M, et al. Mechanisms underlying FeCl3-induced arterial thrombosis. J Thromb Haemost 2011;9 (04):779–789
7 Woollard KJ, Sturgeon S, Chin-Dusting JP, Salem HH, Jackson SP. Erythrocyte hemolysis and hemoglobin oxidation promote ferric chloride-induced vascular injury. J Biol Chem 2009;284(19): 13110–13118
8 Bender M, Hagedorn I, Nieswandt B. Genetic and antibody-induced glycoprotein VI deficiency equally protects mice from mechanically and FeCl(3) -induced thrombosis. J Thromb Haemost 2011;9(07):1423–1426
9 Konstantinides S, Ware J, Marchese P, Almus-Jacobs F, Loskutoff DJ, Ruggeri ZM. Distinct antithrombotic consequences of platelet glycoprotein Ibalpha and VI deficiency in a mouse model of arterial thrombosis. J Thromb Haemost 2006;4(09):2014–2021
10 Kuijpers MJ, Gilio K, Reitsma S, et al. Complementary roles of platelets and coagulation in thrombus formation on plaques acutely ruptured by targeted ultrasound treatment: a novel intravital model. J Thromb Haemost 2009;7(01):152–161
11 Kuijpers MJ, Heemskerk JW. Intravital imaging of thrombus formation in small and large mouse arteries: experimentally induced vascular damage and plaque rupture in vivo. Methods Mol Biol 2012;788:3–19
12 Koizumi J, Yoshida Y, Nakazawa T, Ooneda G. Experimental studies of ischemic brain edema. I. A new experimental model of cerebral embolism in rats in which recirculation can be introduced in the ischemic area. Jpn Stroke J 1986;8:1–8. Doi: 10.3995/jstroke.8.1
13 Longa EZ, Weinstein PR, Carlson S, Cummins R. Reversible middle cerebral artery occlusion without craniectomy in rats. Stroke 1989;20(01):84–91
14 Braeuninger S, Kleinschnitz C, Nieswandt B, Stoll G. Focal cerebral ischemia. Methods Mol Biol 2012;788:29–42
15 Canazza A, Minati L, Boffano C, Parati E, Binks S. Experimental models of brain ischemia: a review of techniques, magnetic resonance imaging, and investigational cell-based therapies. Front Neurol 2014;5:19
16 Howells DW, Porritt MJ, Rewell SS, et al. Different strokes for different folks: the rich diversity of animal models of focal cerebral ischemia. J Cereb Blood Flow Metab 2010;30(08): 1412–1431
17 Bederson JB, Pitts LH, Tsuji M, Nishimura MC, Davis RL, Bartkowski H. Rat middle cerebral artery occlusion: evaluation of the model and development of a neurologic examination. Stroke 1986;17(03):472–476
18 Moran PM, Higgins LS, Cordell B, Moser PC. Age-related learning deficits in transgenic mice expressing the 751-amino acid isoform of human beta-amyloid precursor protein. Proc Natl Acad Sci U S A 1995;92(12):5341–5345
19 Mizuma A, You JS, Yenari MA. Targeting reperfusion injury in the age of mechanical thrombectomy. Stroke 2018;49(07): 1796–1802
20 Stoll G, Nieswandt B. Thrombo-inflammation in acute ischaemic stroke - implications for treatment. Nat Rev Neurol 2019;15(08): 473–481
21 Nieswandt B, Kleinschnitz C, Stoll G. Ischaemic stroke: a thrombo-inflammatory disease? J Physiol 2011;589(17): 4115–4123
22 Kleinschnitz C, Pozgajova M, Pham M, Bendszus M, Nieswandt B, Stoll G. Targeting platelets in acute experimental stroke: impact of glycoprotein Ib, VI, and IIb/IIIa blockade on infarct size, functional outcome, and intracranial bleeding. Circulation 2007;115(17):2323–2330
23 Deppermann C, Cherpokova D, Nurden P, et al. Gray platelet syndrome and defective thrombo-inflammation in Nbeal2-deficient mice. J Clin Invest 2013;123(08):3331–3342
24 Stegner D, Deppermann C, Kraft P, et al. Munc13-4-mediated secretion is essential for infarct progression but not intracranial

hemostasis in acute stroke. J Thromb Haemost 2013;11(07): 1430–1433
25 Dong X, Gao J, Zhang CY, Hayworth C, Frank M, Wang Z. Neutrophil membrane-derived nanovesicles alleviate inflammation to protect mouse brain injury from ischemic stroke. ACS Nano 2019;13(02):1272–1283
26 Mostany R, Portera-Cailliau C. A craniotomy surgery procedure for chronic brain imaging. J Vis Exp 2008;(12):680
27 Desilles JP, Loyau S, Syvannarath V, et al. Alteplase reduces downstream microvascular thrombosis and improves the benefit of large artery recanalization in stroke. Stroke 2015;46(11): 3241–3248
28 Göb V, Voll MG, Zimmermann L, et al. Infarct growth precedes cerebral thrombosis following experimental stroke in mice. Sci Rep 2021;11(01):22887
29 Ishikawa M, Vowinkel T, Stokes KY, et al. CD40/CD40 ligand signaling in mouse cerebral microvasculature after focal ischemia/reperfusion. Circulation 2005;111(13):1690–1696
30 Bonnard T, Hagemeyer CE. Ferric chloride-induced thrombosis mouse model on carotid artery and mesentery vessel. J Vis Exp 2015;(100):e52838
31 Zhang Y, Ye J, Hu L, et al. Increased platelet activation and thrombosis in transgenic mice expressing constitutively active P2Y12. J Thromb Haemost 2012;10(10):2149–2157
32 Munnix IC, Strehl A, Kuijpers MJ, et al. The glycoprotein VI-phospholipase Cgamma2 signaling pathway controls thrombus formation induced by collagen and tissue factor in vitro and in vivo. Arterioscler Thromb Vasc Biol 2005;25(12):2673–2678
33 Rybaltowski M, Suzuki Y, Mogami H, et al. In vivo imaging analysis of the interaction between unusually large von Willebrand factor multimers and platelets on the surface of vascular wall. Pflugers Arch 2011;461(06):623–633
34 Leung FW, Su KC, Pique JM, Thiefin G, Passaro E Jr, Guth PH. Superior mesenteric artery is more important than inferior mesenteric artery in maintaining colonic mucosal perfusion and integrity in rats. Dig Dis Sci 1992;37(09):1329–1335
35 Collard CD, Gelman S. Pathophysiology, clinical manifestations, and prevention of ischemia-reperfusion injury. Anesthesiology 2001;94(06):1133–1138
36 Abela CB, Homer-Vanniasinkham S. Clinical implications of ischaemia-reperfusion injury. Pathophysiology 2003;9(04):229–240
37 Parks DA, Granger DN. Contributions of ischemia and reperfusion to mucosal lesion formation. Am J Physiol 1986;250(6, Pt 1): G749–G753
38 Cicalese L, Iyengar A, Subbotin V, et al. Protection afforded by pyruvate during acute rejection of small-bowel allografts is mediated by inhibition of oxygen-free radicals and cytolytic activity (perforin and granzyme-B mRNA expression) in activated leukocytes. Transplant Proc 1997;29(1-2):704
39 Thorburn T, Aali M, Lehmann C. Immune response to systemic inflammation in the intestinal microcirculation. Front Biosci 2018;23(04):782–795
40 Bayer F, Ascher S, Kiouptsi K, Kittner JM, Stauber RH, Reinhardt C. Colonization with altered Schaedler flora impacts leukocyte adhesion in mesenteric ischemia-reperfusion injury. Microorganisms 2021;9(08):1601
41 Ascher S, Wilms E, Pontarollo G, et al. Gut microbiota restricts NETosis in acute mesenteric ischemia-reperfusion injury. Arterioscler Thromb Vasc Biol 2020;40(09):2279–2292
42 Grover SP, Bendapudi PK, Yang M, et al. Injury measurements improve interpretation of thrombus formation data in the cremaster arteriole laser-induced injury model of thrombosis. J Thromb Haemost 2020;18(11):3078–3085
43 Falati S, Gross P, Merrill-Skoloff G, Furie BC, Furie B. Real-time in vivo imaging of platelets, tissue factor and fibrin during arterial thrombus formation in the mouse. Nat Med 2002;8(10):1175–1181
44 Chou J, Mackman N, Merrill-Skoloff G, Pedersen B, Furie BC Furie B. Hematopoietic cell-derived microparticle tissue factor contributes to fibrin formation during thrombus propagation. Blood 2004;104(10):3190–3197
45 Duan X, Perveen R, Dandamudi A, et al. Pharmacologic targeting of Cdc42 GTPase by a small molecule Cdc42 activity-specific inhibitor prevents platelet activation and thrombosis. Sci Rep 2021;11(01):13170
46 Dubois C, Panicot-Dubois L, Gainor JF, Furie BC, Furie B. Thrombin-initiated platelet activation in vivo is vWF independent during thrombus formation in a laser injury model. J Clin Invest 2007;117(04):953–960
47 Atkinson BT, Jasuja R, Chen VM, Nandivada P, Furie B, Furie BC. Laser-induced endothelial cell activation supports fibrin formation. Blood 2010;116(22):4675–4683
48 Neyman M, Gewirtz J, Poncz M. Analysis of the spatial and temporal characteristics of platelet-delivered factor VIII-based clots. Blood 2008;112(04):1101–1108
49 Mangin P, Yap CL, Nonne C, et al. Thrombin overcomes the thrombosis defect associated with platelet GPVI/FcRgamma deficiency. Blood 2006;107(11):4346–4353
50 Mitrophanov AY, Merrill-Skoloff G, Grover SP, et al. Injury length and arteriole constriction shape clot growth and blood-flow acceleration in a mouse model of thrombosis. Arterioscler Thromb Vasc Biol 2020;40(09):2114–2126
51 Stolla M, Stefanini L, Roden RC, et al. The kinetics of αIIbβ3 activation determines the size and stability of thrombi in mice: implications for antiplatelet therapy. Blood 2011;117(03): 1005–1013
52 Gromotowicz-Poplawska A, Flaumenhaft R, Gholami SK, et al. Enhanced thrombotic responses are associated with Striatin deficiency and aldosterone. J Am Heart Assoc 2021;10(22): e022975
53 Revollo L, Merrill-Skoloff G, De Ceunynck K, et al. The secreted tyrosine kinase VLK is essential for normal platelet activation and thrombus formation. Blood 2022;139(01):104–117
54 Lutsey PL, Zakai NA. Epidemiology and prevention of venous thromboembolism. Nat Rev Cardiol 2023;20(04):248–262
55 López JA, Chen J. Pathophysiology of venous thrombosis. Thromb Res 2009;123(Suppl 4):S30–S34
56 Wang X, Smith PL, Hsu MY, Ogletree ML, Schumacher WA. Murine model of ferric chloride-induced vena cava thrombosis: evidence for effect of potato carboxypeptidase inhibitor. J Thromb Haemost 2006;4(02):403–410
57 Witsch T, Mauler M, Herr N, et al. A novel hollow and perforated flexible wire allows the safe and effective local application of thrombolytic therapy in a mouse model of deep vein thrombosis. J Thromb Thrombolysis 2014;37(04):450–454
58 Esmon CT. Basic mechanisms and pathogenesis of venous thrombosis. Blood Rev 2009;23(05):225–229
59 Payne H, Brill A. Stenosis of the inferior vena cava: a murine model of deep vein thrombosis. J Vis Exp 2017;(130):56697
60 Wrobleski SK, Farris DM, Diaz JA, Myers DD Jr, Wakefield TW. Mouse complete stasis model of inferior vena cava thrombosis. J Vis Exp 2011;(52):2738
61 Wakefield TW, Strieter RM, Wilke CA, et al. Venous thrombosis-associated inflammation and attenuation with neutralizing antibodies to cytokines and adhesion molecules. Arterioscler Thromb Vasc Biol 1995;15(02):258–268
62 von Brühl ML, Stark K, Steinhart A, et al. Monocytes, neutrophils, and platelets cooperate to initiate and propagate venous thrombosis in mice in vivo. J Exp Med 2012;209(04):819–835
63 Mwiza JMN, Lee RH, Paul DS, et al. Both G protein-coupled and immunoreceptor tyrosine-based activation motif receptors mediate venous thrombosis in mice. Blood 2022;139(21):3194–3203
64 Schönfelder T, Jäckel S, Wenzel P. Mouse models of deep vein thrombosis. Gefasschirurgie 2017;22(Suppl 1):28–33
65 Diaz JA, Obi AT, Myers DD Jr, et al. Critical review of mouse models of venous thrombosis. Arterioscler Thromb Vasc Biol 2012;32(03):556–562

66 Brandt M, Schönfelder T, Schwenk M, et al. Deep vein thrombus formation induced by flow reduction in mice is determined by venous side branches. Clin Hemorheol Microcirc 2014;56(02): 145–152
67 Geddings J, Aleman MM, Wolberg A, von Brühl ML, Massberg S, Mackman N. Strengths and weaknesses of a new mouse model of thrombosis induced by inferior vena cava stenosis: communication from the SSC of the ISTH. J Thromb Haemost 2014;12(04): 571–573
68 Stark K, Massberg S. Interplay between inflammation and thrombosis in cardiovascular pathology. Nat Rev Cardiol 2021; 18(09):666–682
69 Beristain-Covarrubias N, Perez-Toledo M, Thomas MR, Henderson IR, Watson SP, Cunningham AF. Understanding infection-induced thrombosis: lessons learned from animal models. Front Immunol 2019;10:2569
70 Hitchcock JR, Cook CN, Bobat S, et al. Inflammation drives thrombosis after Salmonella infection via CLEC-2 on platelets. J Clin Invest 2015;125(12):4429–4446
71 Beristain-Covarrubias N, Perez-Toledo M, Flores-Langarica A, et al. *Salmonella*-induced thrombi in mice develop asynchronously in the spleen and liver and are not effective bacterial traps. Blood 2019;133(06):600–604
72 Levi M, Ten Cate H. Disseminated intravascular coagulation. N Engl J Med 1999;341(08):586–592
73 van der Poll T, Opal SM. Host-pathogen interactions in sepsis. Lancet Infect Dis 2008;8(01):32–43
74 van der Poll T, van de Veerdonk FL, Scicluna BP, Netea MG. The immunopathology of sepsis and potential therapeutic targets. Nat Rev Immunol 2017;17(07):407–420
75 Berube BJ, Bubeck Wardenburg J. *Staphylococcus aureus* α-toxin: nearly a century of intrigue. Toxins (Basel) 2013;5 (06):1140–1166
76 Parimon T, Li Z, Bolz DD, et al. *Staphylococcus aureus* α-hemolysin promotes platelet-neutrophil aggregate formation. J Infect Dis 2013;208(05):761–770
77 Surewaard BGJ, Thanabalasuriar A, Zeng Z, et al. α-Toxin induces platelet aggregation and liver injury during *Staphylococcus aureus* sepsis. Cell Host Microbe 2018;24(02):271–284.e3
78 Surewaard BGJ, Kubes P. Measurement of bacterial capture and phagosome maturation of Kupffer cells by intravital microscopy. Methods 2017;128:12–19
79 Agopian VG, Harlander-Locke MP, Markovic D, et al. Evaluation of early allograft function using the liver graft assessment following transplantation risk score model. JAMA Surg 2018;153(05): 436–444
80 Eltzschig HK, Eckle T. Ischemia and reperfusion – from mechanism to translation. Nat Med 2011;17(11):1391–1401
81 Zhai Y, Petrowsky H, Hong JC, Busuttil RW, Kupiec-Weglinski JW. Ischaemia-reperfusion injury in liver transplantation – from bench to bedside. Nat Rev Gastroenterol Hepatol 2013;10(02): 79–89
82 Selzner M, Selzner N, Jochum W, Graf R, Clavien P-A. Increased ischemic injury in old mouse liver: an ATP-dependent mechanism. Liver Transpl 2007;13(03):382–390
83 Guan L-Y, Fu PY, Li PD, et al. Mechanisms of hepatic ischemia-reperfusion injury and protective effects of nitric oxide. World J Gastrointest Surg 2014;6(07):122–128
84 Brenner C, Galluzzi L, Kepp O, Kroemer G. Decoding cell death signals in liver inflammation. J Hepatol 2013;59(03):583–594
85 Nakamura K, Kageyama S, Ke B, et al. Sirtuin 1 attenuates inflammation and hepatocellular damage in liver transplant ischemia/Reperfusion: from mouse to human. Liver Transpl 2017;23(10):1282–1293
86 Zhang XJ, Cheng X, Yan ZZ, et al. An ALOX12-12-HETE-GPR31 signaling axis is a key mediator of hepatic ischemia-reperfusion injury. Nat Med 2018;24(01):73–83
87 Li P, He K, Li J, Liu Z, Gong J. The role of Kupffer cells in hepatic diseases. Mol Immunol 2017;85:222–229
88 Zhang J, Xu P, Song P, et al. CCL2-CCR2 signaling promotes hepatic ischemia/reperfusion injury. J Surg Res 2016;202(02): 352–362
89 Yang X, Liang L, Zong C, et al. Kupffer cells-dependent inflammation in the injured liver increases recruitment of mesenchymal stem cells in aging mice. Oncotarget 2016;7(02): 1084–1095
90 Lai X, Gong J, Wang W, et al. Acetyl-3-aminoethyl salicylate ameliorates hepatic ischemia/reperfusion injury and liver graft survival through a high-mobility group box 1/toll-like receptor 4-dependent mechanism. Liver Transpl 2019;25(08): 1220–1232
91 de Oliveira THC, Marques PE, Poosti F, et al. Intravital microscopic evaluation of the effects of a CXCR2 antagonist in a model of liver ischemia reperfusion injury in mice. Front Immunol 2018; 8:1917
92 Faust N, Varas F, Kelly LM, Heck S, Graf T. Insertion of enhanced green fluorescent protein into the lysozyme gene creates mice with green fluorescent granulocytes and macrophages. Blood 2000;96(02):719–726
93 Marques PE, Oliveira AG, Chang L, Paula-Neto HA, Menezes GB. Understanding liver immunology using intravital microscopy. J Hepatol 2015;63(03):733–742
94 Cywes R, Packham MA, Tietze L, et al. Role of platelets in hepatic allograft preservation injury in the rat. Hepatology 1993;18(03): 635–647
95 Cywes R, Mullen JB, Stratis MA, et al. Prediction of the outcome of transplantation in man by platelet adherence in donor liver allografts. Evidence of the importance of prepreservation injury. Transplantation 1993;56(02):316–323
96 Yadav SS, Howell DN, Steeber DA, Harland RC, Tedder TF, Clavien P-A. P-Selectin mediates reperfusion injury through neutrophil and platelet sequestration in the warm ischemic mouse liver. Hepatology 1999;29(05):1494–1502
97 Khandoga A, Biberthaler P, Messmer K, Krombach F. Platelet-endothelial cell interactions during hepatic ischemia-reperfusion in vivo: a systematic analysis. Microvasc Res 2003;65(02): 71–77
98 Tedder TF, Steeber DA, Chen A, Engel P. The selectins: vascular adhesion molecules. FASEB J 1995;9(10):866–873
99 Khandoga A, Biberthaler P, Enders G, et al. P-selectin mediates platelet-endothelial cell interactions and reperfusion injury in the mouse liver in vivo. Shock 2002;18(06):529–535
100 Mende K, Reifart J, Rosentreter D, et al. Targeting platelet migration in the postischemic liver by blocking protease-activated receptor 4. Transplantation 2014;97(02):154–160
101 Khandoga A, Biberthaler P, Enders G, et al. Platelet adhesion mediated by fibrinogen-intercellular adhesion molecule-1 binding induces tissue injury in the postischemic liver in vivo. Transplantation 2002;74(05):681–688
102 Jaeschke H. Molecular mechanisms of hepatic ischemia-reperfusion injury and preconditioning. Am J Physiol Gastrointest Liver Physiol 2003;284(01):G15–G26
103 Gow AJ, Thom SR, Ischiropoulos H. Nitric oxide and peroxynitrite-mediated pulmonary cell death. Am J Physiol 1998;274 (01):L112–L118
104 Selzner N, Rudiger H, Graf R, Clavien PA. Protective strategies against ischemic injury of the liver. Gastroenterology 2003;125 (03):917–936
105 Vodovotz Y, Kim PK, Bagci EZ, et al. Inflammatory modulation of hepatocyte apoptosis by nitric oxide: in vivo, in vitro, and in silico studies. Curr Mol Med 2004;4(07):753–762
106 Lesurtel M, Graf R, Aleil B, et al. Platelet-derived serotonin mediates liver regeneration. Science 2006;312(5770):104–107

107 Nocito A, Georgiev P, Dahm F, et al. Platelets and platelet-derived serotonin promote tissue repair after normothermic hepatic ischemia in mice. Hepatology 2007;45(02):369–376
108 Zhang H, Goswami J, Varley P, et al. Hepatic surgical stress promotes systemic immunothrombosis that results in distant organ injury. Front Immunol 2020;11:987
109 Panteleev MA, Korin N, Reesink KD, et al. Wall shear rates in human and mouse arteries: standardization of hemodynamics for in vitro blood flow assays: communication from the ISTH SSC subcommittee on biorheology. J Thromb Haemost 2021;19(02):588–595
110 Allan-Rahill NH, Lamont MRE, Chilian WM, Nishimura N, Small DM. Intravital microscopy of the beating murine heart to understand cardiac leukocyte dynamics. Front Immunol 2020; 11:92
111 Kalia N. A historical review of experimental imaging of the beating heart coronary microcirculation in vivo. J Anat 2023; 242(01):3–16
112 Mahmoud O, El-Sakka M, Janssen BGH. Two-step machine learning method for the rapid analysis of microvascular flow in intravital video microscopy. Sci Rep 2021;11(01):10047